C. Brault, C. Gil, A. Boboc, P. Spuig
and JET EFDA contributors

Evaluation of the Faraday Angle by Numerical Methods and Comparison with the Tore Supra and JET Polarimeter Electronics

Evaluation of the Faraday Angle by Numerical Methods and Comparison with the Tore Supra and JET Polarimeter Electronics

C. Brault[1], C. Gil[1], A. Boboc[2], P. Spuig[1]
and JET EFDA contributors*

ABSTRACT

On the Tore Supra tokamak, a Far InfraRed (FIR) polarimeter diagnostic has been routinely used for diagnosing the current density by measuring the Faraday rotation angle.

A high precision of measurement is needed to correctly reconstruct the current profile. To reach this precision, electronics used to compute the phase and the amplitude of the detected signals must have a good resilience of the noise present in the measurement chain.

In this article, we analyse the way the analogue cards response to the noise coming from the detectors and their impact on the Faraday angle measurements, and we present numerical methods to calculate the phase and the amplitude. These validations have been done by using real signals acquired by Tore Supra and JET experiments.

These methods have been developed to be used in real-time in the future numerical cards that will replace the Tore Supra present analogue ones.

1. INTRODUCTION

In magnetic fusion, the poloidal current control is a key factor to optimize the confinement and thus to reach the Lawson criteria. FIR polarimetric diagnostics have been developed to allow measurement of this current but still need to be improved to reach the required precisions and reliability.

On Tore Supra, the present accuracy of the polarimeter is about 0.2^{o}, for an operating range of around 20 degrees for the Faraday rotation angle. To be useful to a correct current profiles reconstruction, the accuracy needs to reach 0.05^{o} [1]. This corresponds to 0.2^{o} accuracy for tokamaks with Faraday angles of the order of 40° like JET [2] and in the future ITER [3].

This article describes the present analogue electronic cards used on Tore Supra, and compares the experimental signals carried out by the cards with numerical Matlab simulations, for Tore Supra and JET. Real time methods of calculation to be embedded in numerical electronics are also discussed.

2. PRINCIPLE OF THE POLARIMETRY

On Tore Supra, the method used to determine the polarisation of the beam (Figure 1) appeals to a two detector technique [4][5]: a linear polarised laser beam of wavelength of 195µm (Deuterated Cyanide laser source) incoming linearly polarised beam crosses the plasma that it is optically active. The interaction with its magnetic field along the propagation direction causes a rotation of the polarisation plane, this being called the Faraday rotation effect. The Faraday angle can be approximated by the following expression [6]:

$$\Psi_P = C\,\lambda^2 \int n_e\,B_{//}\ dz$$

Where λ is the wavelength, ne the electron density, $B_{//}$ the magnetic field parallel to the beam propagation, C a constant and the integral is extended over the beam path [4]. By inversion of this integral relation, the poloidal magnetic field and consequently the current density profile can be deduced.

But plasma has also birefringence properties and the beams are affected by the Cotton-Mouton effect [4]. In optical terms this means that the beam becomes elliptically polarised as well. Electronically the two orthogonal components of the rotated elliptical beam are shifted and this phase shift is sensitive to the square of the magnetic field $B_\perp$ perpendicular to the propagation as follows:

$$\alpha_F = C.\lambda^2 . \int n_e B_{//}.dz$$

After having crossed the plasma, the probe beam is then recombined with a 100kHz frequency shifted beam. A free standing wire grid separates the two perpendicular polarisation components before they reach the two detectors. The detectors are semi-conductor InSb bolometers that are implanted in helium-cooled cryostats. They are only sensitive to the 100kHz interference component between the two beams.

The rotation of the polarization induces changes of amplitudes that are measured on the detectors. This method needs a calibration set, which is constituted of a half wavelength quartz plate, to evaluate the response of the detectors to a known rotation.

The main difficulty of this technique is to avoid spurious differential misalignments between the two detectors during plasmas that lead to different relative amplitudes. They can be induced by the moves of mirrors or plasma refraction. This imposes to install the grid as near as possible at an equal distance from the detectors. The minimal distance from the grid to the detector is presently typically 50 centimetres on Tore Supra [7].

When a linearly polarised incident wave (the probing beam) crosses the magnetized plasma, its state of polarisation changes by combination the Faraday and the Cotton-Mouton effects. This state of polarisation can be fully described by two equivalent couples of angles (Figure 2):

- ψ_P the azimuth, angle between the ellipse major axis and the X direction, and χ_P the ellipticity, angle given by the major and the minor axis (independent coordinate), and
- θ_P the elevation, angle given by the maxima of the two components on X and Y, and ϕ_P the phase difference between them.

As the Faraday rotation angle is at most twenty degrees on Tore Supra, the equations of the ellipse can be linearized:

$$\Psi_P \approx \theta_P .\cos(\phi_P) \approx \frac{B}{A}\cos(\phi_P) = \frac{AB\cos(\phi_P)}{A^2}$$

where A and B are the amplitude of the first and second signal coming from the detectors respectively.

The Faraday angle is theoretically deduced from the measurement of $ABcos(\phi_P)$ and A^2. But a constant residual phase difference ϕ_0 exists in the diagnostic, due the optics and the electronic cards. The measured phase difference is no more ϕ_P but $(\phi_P - \phi_0)$, giving a new formula:

$$\psi_P \approx \frac{AB \cos(\phi_P - \phi_0)}{A^2} = \frac{AB \cos(\phi_P)}{A^2}\cos(\phi_0)... \quad ... + \frac{AB \sin(\phi_P)}{A^2}\sin(\phi_0)$$

2

This phase difference ϕ_0 is calculated during the diagnostic calibration, as well as calibration coefficients K_i (by 3rd degree polynomial fit [8]) to correct the losses due to the optics and the detector response:

$$\Psi_P \approx \sum_{i=1}^{3} K_i \cdot \left[\frac{AB\cos(\phi_P - \phi_0)}{A^2} \right]^i$$

3. THEANALOGUE ELECTRONIC CARDS USED ONTORE SUPRA AND JET

3.1. TORE SUPRA

The electronic cards have been designed to calculate in real-time the phase ϕ_P and the amplitudes A and B from 100kHz signals measured by the detectors, which can be written $A.\cos(\omega t)$ and $B.\cos(\omega t + \phi_P)$.

The Figure 3 shows the different ways used on the electronic cards to calculate the four output signals. The cards don't calculate directly A^2 and B^2 signals, but A and B signals. These amplitudes are obtained by using a RMS-to-DC converter (AD536), while $A.B.\cos(\phi_P)$ and $A.B.\sin(\phi_P)$ are calculated by synchronous multiplication (by an analogue multiplier AD633) and 1kHz low pass filtering (to keep only the constant part of the signal).

To obtain $A.B.\sin(\phi_P)$, the first input signal $A.\cos(wt+fP)$ is phase shifted of 90°, in order to become $A.\sin(\omega t + \phi_P)$. This operation is made by an integrator (based on operational amplifier OP27). An automatic gain correction is performed to take into account the integrator response by comparing the RMS-to-DC measurement of the A signal before and after the integration

3.2. JET

The JET electronics is very similar to the Tore Supra one, using synchronous amplifiers and filters, except that is calculated the square of the amplitude of the probing beam, by multiplying the signal by itself and then filtering. The sin is also obtained by first phase shifting the probe signal then uses the synchronous amplifier and filtering method. The square of the amplitude after the integration is also calculated and is an output.

The two 100kHz signals used on JET can be written [9]:

$$i(t) = E_X \cos(\omega t)$$
$$p(t) = E_Y \cos(\omega t - \phi)$$

Where E_X and E_Y are the amplitude, ω the pulsation of the probing beam and ϕ the phase between the two signals. The analogue electronic cards evaluate the signals by multiplication and integration according to

$$\text{PSD} = \langle p(t) \times i(t) \rangle \ (\propto E_X E_Y \cos\phi)$$
$$\text{PSP} = \langle p(t) \times i'(t) \rangle \ (\propto E'_X E_Y \cos\phi)$$
$$\text{RMS} = \langle i(t) \times i(t) \rangle \ (\propto E_X^2)$$
$$\text{RMS} = \langle i'(t) \times i'(t) \rangle \ (\propto E_X'^2)$$

Where $i'(t)$ is obtained from $i(t)$ by a phase shift of 90°. From these signals, two ratios are used to calculate the phase and the faraday angle:

$$R = \frac{PSD}{RMS} \qquad R' = \frac{PSP}{\sqrt{RMS.RMP}}$$

The Faraday angle is then calculated with the formula in the ideal polarimeter scheme:

$$\Psi_P = C \arctan (R'/R)$$

Where C is the calibration factor.

4. NUMERICALMETHODS

The numerical calculations have been done in a first time for the comparison with the analogue card outputs. These methods have then evolved to be usable in real-time numerical cards.

The Figure 4 shows these methods used to calculate the same signals as the analogue electronic card ones. The first step is to digitalize the analogue signal. To have a good precision, we need to choose a sampling rate higher than the frequency of the studied signal.

As the beam frequency is around 100kHz, we have chosen a sampling frequency of 1MHz.

The A^2 or B^2 values are obtained by a direct multiplication of the digitalized signal by itself, and then by a filtering of the result. For filtering, we use a 1000 point smooth function. A lowpass filter can be used as well but this would lead to a gain modification that has to be taken into account.

The $A.B.cos(\phi_P)$ signal is calculated by the same method, by multiplying the two input signals and filtering.

The calculation of $A.B.sin(\phi_P)$ is less straightforward. A first possible method is to interpolate the second input signal to calculate the signal a quarter of its period later. A cosine signal is thus transformed into a sine signal.

This method by interpolation presents defaults due to sampling frequency sensitivity. With a 1MHz sampling rate, the error on the amplitude of the phase shifted signal can reach more than 4.5% (see Table 1), which is incompatible with the precision to be achieved.

This error can be reduced if we choose an option for the interpolation function in Matlab, as an example 'spline' or 'cubic', but this solution cannot be easily programmed on a numerical processing card.

Thus, we developed an other numerical method based on an N points shift of the digitalized signal. This method is shown on Figure 5.

From the original time t_1 and the corresponding points M_1 and M_3 of the digitalized signals, we then choose a second time t_2 and the corresponding point M_2 on the first digitalized signal (which can be either $A.cos(\omega t)$ or $B.cos(\omega t + \phi_P)$, this method is symmetrical). If this point M_2 is the next of M_1 in the digitalized signal, we obtain a 1 point shift (N=1).

With these three points, we can calculate all the signals needed to evaluate the Faraday angle:

$$A^2 = 2 \times \langle M_1.M_1 \rangle$$

$$AB\cos(\Phi_P) = 2 \times \langle M_1.M_3 \rangle$$

$$AB\sin(\Phi_P) = \frac{\langle M_1.M_3 \rangle.\cos[\omega.(t_2 - t_1)] - \langle M_2.M_3 \rangle}{\sin[\omega.(t_2 - t_1)]}$$

Where ω is the known modulation of the signal. The precision on the calculated signal of this method is higher than the interpolation's one (Table 2). With this method, we obtain an error never worse than 2.10^{-5} % according to the sampling rate or the number of points for the shift, to be compared with the error up to 5% for the interpolation method. Another advantage of this calculation is that can be easily programmed in a numerical card.

5. NOISE STUDYAND NUMERICALCALCULATIONS

To reach a precision of 0.05^o on the Faraday rotation angle measurement, and correctly reconstruct the current profile, we studied the way the analogue electronic cards deal with almost perfect generator delivered signals and with real noisy signals coming from the detectors.

5.1. TESTS OF THE TORE SUPRA ANALOGUE CARDS WITH GENERATORS.

The first tests of the analogue cards of Tore Supra have consisted in verifying the error on each channel with input signals delivered by a generator. These tests have been done in a laboratory. We have performed three tests for each channel of the cards, by changing the values of A, B and fP and the results are presented in the Table 3.

The maximum measured error is 1.2% on the A channel. This error is compatible with the wanted precision chosen when the cards have been designed.

For the third test, we have added an artificial white noise on the second input signal to verify the impact on the measurement. According to the results of this test, the analogue cards have not been affected by this noise, the maximum error in this case is 1.1%.

These first tests have shown that the analogue cards deals correctly the generator signals in laboratory, even with added noise.

5.2. TESTS WITH TORE SUPRA REAL SIGNALS

On Tore Supra, the sampling rate of data recording is 1kHz, not allowing a correct study of noise on the different channels of the cards. To carry out this study, experimental input and output signals have been recorded by a Yokogawa oscilloscope (1MHz sampling rate, 10s duration) on the channel 3 of the polarimeter. The records have been done during the calibration and the plasma pulse, where the amplitude variations are very important (during the calibration, a half-wavelength plate rotates from -15° to $+15^o$ to simulate the rotation of the polarisation of the probing beam).

Contrary to the laboratory tests presented in the previous paragraph, during these records the cards are in their experimental rack in the Tore Supra Hall environment.

On Figure 6 are shown the results of these records and calculations. On the figure are represented the records of the *A, ABcos*(ϕ_P) and *ABsin*(ϕ_P) (in blue) and the results of the Matlab simulations (in red). *ABsin*(ϕ_P) has been calculated with a 1 point shift (corresponding to shift of a tenth of the period). For each signal, a zoom is present to compare the level of noise for both signals.

The Figure 6a represents the experimental and calculated A signals. In the zoom box, we can see that the experimental noise (in blue) on this signal is of the order of 150mV, three times higher than the noise of the calculated signal (in red). Moreover, the mean values of theses two signals are not equal. An approximate 100mV difference around 100mV can be observed.

The maximum amplitude on the experimental signal is 3.8V. According to the equation used to calculate the Faraday angle, the relative error on this angle is 7.9%, which corresponds to a 0.79° error for a Faraday angle equal to 10° (typical value on Tore Supra). This error is higher than the 0.05° precision that we want to reach and must be decreased.

On the Figure 6b are shown the results for *ABcos*(ϕ_P)signal. The experimental noise is around 90mV and again the numerical noise of 40mV is lower than the experimental one. The relative error on this signal is 1.7% which corresponds 0.17^o for a 10° Faraday angle.

This error is lower than the error on the A channel but is still too high.

On this signal, the same mean value difference can be seen between the experimental and the numerical signal.

The results for the last signal, *ABsin*(ϕ_P), can be seen on the Figure 6c. The experimental noise is lower than the noise for A or *ABcos*(ϕ_P), around 30mV. The numerical signal is less noisy (8mV).

A difference of mean values around 100mV can be measured on this figure as well.

The relative error on this signal is 1.2% which corresponds 0.12^o for a 10° Faraday angle.

To globally confirm this error study, the Faraday angle has been calculated from the experimental signals and from the simulated ones. On the Figure 7 is shown the comparison between the two obtained curves. In the same way as the results on the Figure 6, during the calibration, simulated and experimental mean values are different. But on the zoom, the simulated curve is less noisy than the experimental one, confirming a better noise treatment by the numerical calculation of the noisy signal (mainly because of a lower noisy numerical A signal).

The experimental signal fluctuations due to the noise are around 0.4^o, while the simulated one is around 0.03^o, compatible with the aimed 0.05^o precision.

In conclusion of this comparison, one can see a better treatment of the noise by the numerical methods, and a difference of mean values that doesn't appear during the laboratory tests. This difference could be due to the presence in real signals of high frequency noise that is not correctly filtered and treated by the cards.

The noise level on the numerical signals is compatible with the precision we want to reach on the polarimeter. This result leads us to foresee new cards based on these numerical methods. The validation of the numerical calculation method is reinforced by an other comparison: the

conservation of the equality $(ABcos^2 (\phi_P) + ABsin^2 (\phi_P)/ (A^2B^2) = 1$.

This equality must be verified during the calibration (Figure 8a: rotation of the plate: from -6° to +6°) and during the plasma pulse.

For this test, the input signals have been filtered by a numerical pass band 80-120kHz before simulation to increase the precision of the calculation during the calibration when the B amplitude is near zero.

On Figure 8, one can see that for the experimental data, the equality is not verified. An important difference appears during the calibration (b), corresponding to a B value near zero.

The numerical signal is better; its value is 1 except when B is near zero where its value is 0.97. During the plasma the experimental value is around 0.8. The numerical result is better with a value equal to 1.

This result confirms that the numerical treatment is better than the experimental one, but to increase the precision a very efficient initial filtering on the input signals will be needed.

5.3. JET REAL SIGNALS

To validate our numerical calculation methods on a different polarimeter, we have used JET 100kHz signals as an input to our calculations and compared the results with the outputs of the electronics that are stored in the JET database.

In the simulation, the input signals have been filtered using a 4th order numerical 80-120kHz band path filter to reduce the high frequency noise and increase the precision of the calculation.

On Figure 9 are shown the results of the calculations using these JET input signals during the calibration (20-25s) and during plasma pulse (40-65s). Unlike the Tore Supra cards, the JET electronic outputs present a gain and sometimes an offset.

To compare the results of the calculations with the PSD experimental data (Figure 9 left), we have determined this gain by fitting the calibration peak, and adjusted the offset using the time after the calibration, before the plasma (30-40s).

For PSP (Figure 9 right), we have adjusted the offset by using the time after the calibration and before the plasma but the gain have been calculated by fitting the first peak during the plasma (47s) and not by fitting the calibration peak. One can see it remains an unexplained difference during the calibration.

As the numerical simulations have been done with a sampling rate of 1MHz, whilst the JET Database signals have a 1kHz sampling rate, this leads the apparent noise to be more important on the numerical simulation (in blue) than on the experimental one (in red).

For the PSD signal, one can see a good agreement between calculations and experimental data. The global behaviour is the same and only small differences appear during the plasma.

These differences can be due to an initial phase f0 affecting the experimental data and differently calculated by the numerical method.

For the PSP signal, a good agreement can be seen between the blue and the red curve during this

phase but not during the calibration.

Nevertheless, by using the equation given in the paragraph III.b, one can calculate that the error on the Faraday angle measurement, due to these small differences, is around 0.2^{o}.

The second test is the conservation of $(ABcos^2(\phi_P) + ABsin^2(\phi_P)/(A^2B^2)=1$.

On Figure 10 one are shown the results for this calculation. On JET, the B signal is not calculated, so the numerical simulation cannot be compared with the experimental data. But one can see that the equality is quite well verified for simulation during the calibration (t < 25s) and during the plasma pulse (30s < t < 65s), except when B is near zero at t = 54s as the signals are very noisy at the end of this pulse.

CONCLUSIONAND PERSPECTIVES

This comparative study confirms that the electronic cards used on Tore Supra present a too important noise level for the aimed precision. The transition from an analogue to a numerical signal treatment leads to an important decrease of the error committed on the Faraday angle measurement.

The comparison with data elaborated from different polarimeters like the JET one shows that the method is robust enough to be used with signals that would suffer noise degradation due to various causes.

The developed algorithms are simple enough to be programmed on a numerical processing card.

For Tore Supra, a prototype card based on the Fast Processor Gate Array technology is presently in development to validate this real-time numerical method of the Faraday angle measurement. It will be tested to know if its noise level is as satisfying as the numerical 13 simulations that are presented in this article. After tests in laboratory, it will be validated during the 2011 Tore Supra plasma campaign. This new electronics will be then suitable to be used on the other plasma fusion devices that have similar polarimeters.

ACKNOWLEDGEMENTS

REFERENCES
[1]. C. Gil et al, Fusion Science and Technology Vol. **56** Oct. 2009 p 1238
[2]. M. Brombin, A. Boboc, L. Zabeo, A. Murari: Real-time electron density measurements from Cotton–Mouton effect in JET machine, Review of Scientific Instruments **79**, (2008) 10E718
[3]. A.J.H. Donné, M.F. Graswinckel et al: Poloidal Polarimeter for current density measurements in ITER, Review of Scientific Instruments **75**, 11 (2004) 4694-4701
[4]. E. Joffrin, P. Desfrasne, C. Gil, D. Lapeyre : Polarimetry on Tore Supra, EUR-CEA-FC- 1553

– 1995

[5]. D. Elbeze, C. Gil, F. Imbeaux: Integration off the new reflected channels of the Tore Supra polarimeter for current analysis: 33th EPS conference, Roma 2006.

[6]. D. Veron, in Infrared and Millimeter Waves, K. J. Button, Ed., Vol. **2**, Chap. 2 ~1979

[7]. C. Gil, D. Elbeze and al: Retro-reflected Channels of the Tore Supra FIR Interfero- Polarimeter for the long Pulse Operation, Fusion Engineering and Design **56-57** (2001) 969-973

[8]. D. Elbeze, C. Gil, R. Giannella: Proc EPS 2001

[9]. K. Guenther and JET-EFDA contributors: Complete far-infrared polarimetry measurements at JET, 31st EPS conference, London 2004

Sampling rate	1 MHz	2 MHz	5 MHz	10 MHz
Error on $B.sin(\omega t + \phi_P)$	4.98 %	0.81 %	0.04 %	0.01 %

Table 1. Error on the amplitude of the phase shifted B.sin(ωt+φ$_P$) signal according to the sampling rate.

	1 point shift	2 points shift	3 points shift
1 MHz sampling rate	2.10^{-5} %	2.10^{-5} %	8.10^{-5} %
2 MHz sampling rate	4.10^{-6} %	3.10^{-6} %	5.10^{-7} %
10 MHz sampling rate	$1,6.10^{-9}$ %	$1,5.10^{-9}$ %	$1,4.10^{-9}$ %

Table 2. Error on the calculated signal according to the sampling rate and the number of points for the shift.

	Error on A channel	Error on B channel	Error on $ABcos(\phi_P)$ channel	Error on $ABsin(\phi_P)$ channel
Test 1 A = 2.5 V B = 2 V $\phi_P = 20°$	1.2 %	0.5 %	1 %	0.01 %
Test 2 A = 2.5 V B = 2.5 V $\phi_P = 0°$	0.7 %	0.1 %	0.9 %	0.01 %
Test 3 A = 2.5 V B = 2 V (+10% noise) $\phi_P = 20°$	0.2 %	0.2 %	0.9 %	1.1 %

Table 3. Error on the calculated signal according to the sampling rate and the number of points for the shift.
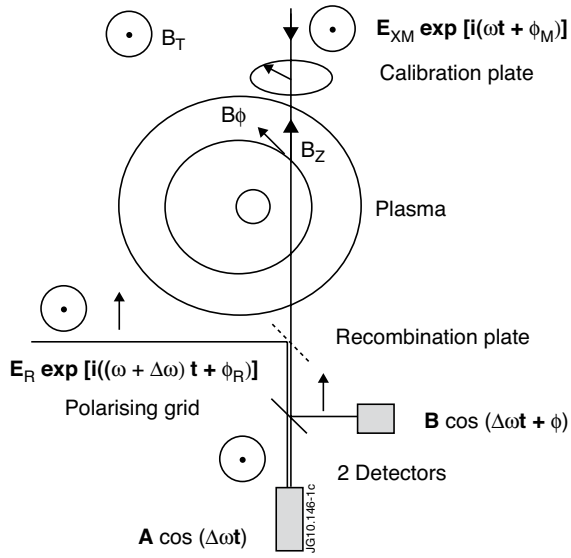
Figure 1. Synoptic of the Tore Supra Polarimeter.

$$\tan \chi_p = \frac{b}{a}$$

$$\tan \theta_p = \frac{B}{A}$$

$$\tan 2\Psi_p = \tan 2\theta_p = \cdot \cos\phi_p$$
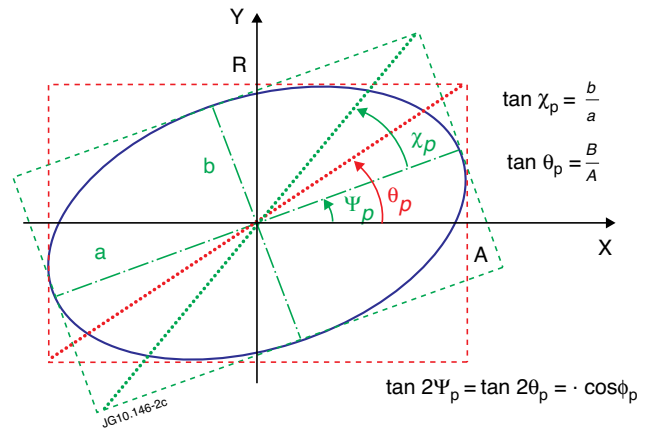
Figure 2. The polarisation ellipse of the probing beam.
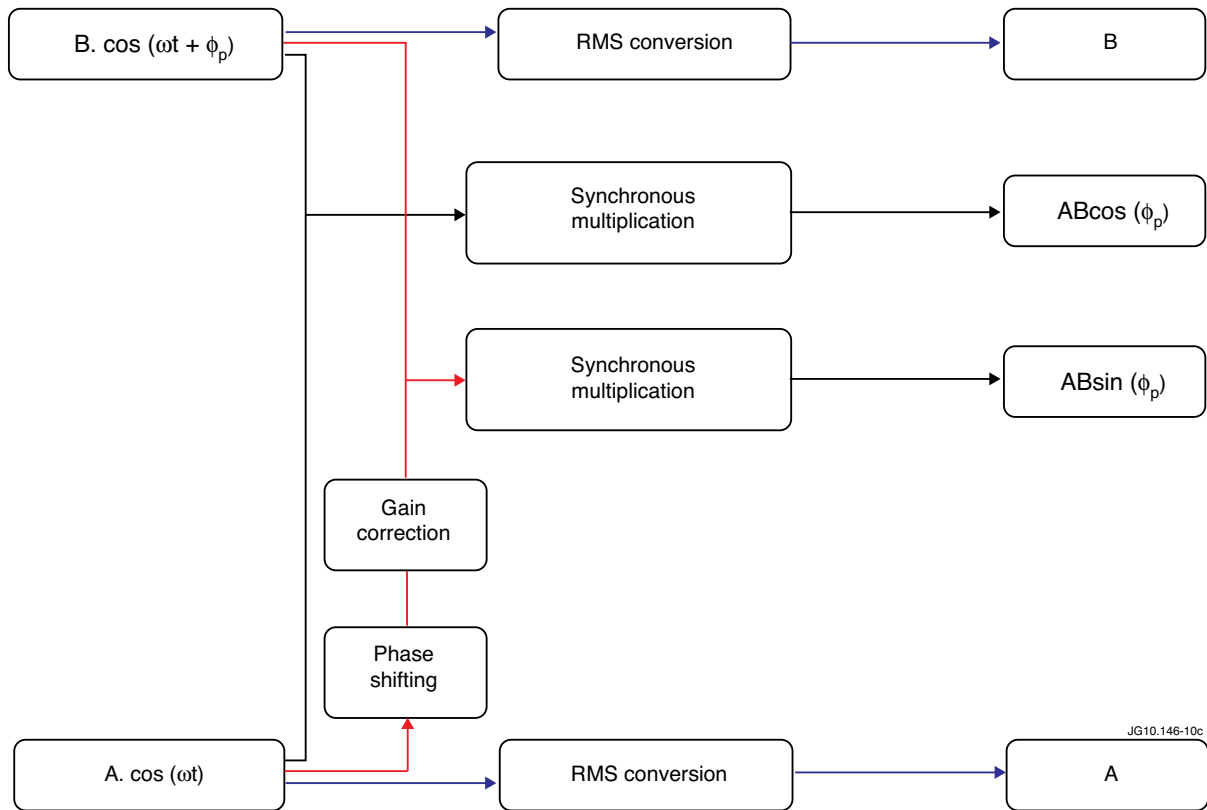
Figure 3: Design of the Tore Supra analogue electronic cards.
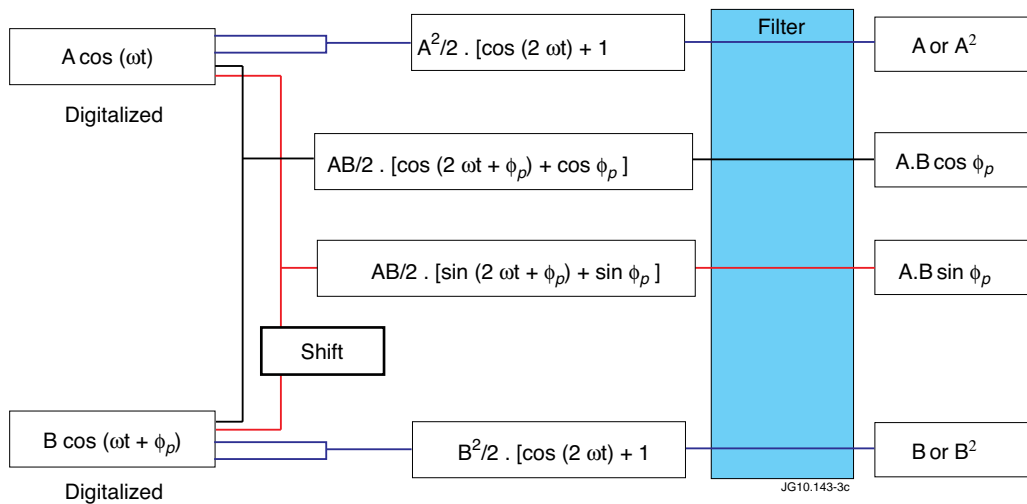
Figure 4. *Numerical methods to calculate the Faraday angle.*
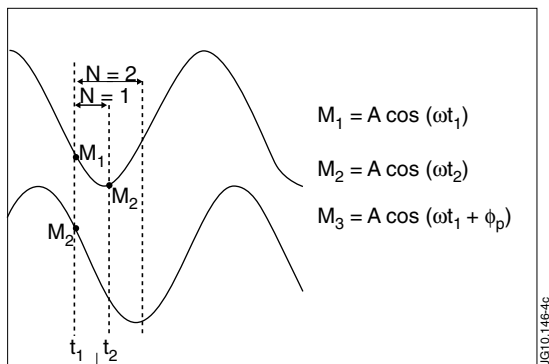
Figure 5. *N point shift calculation method.*
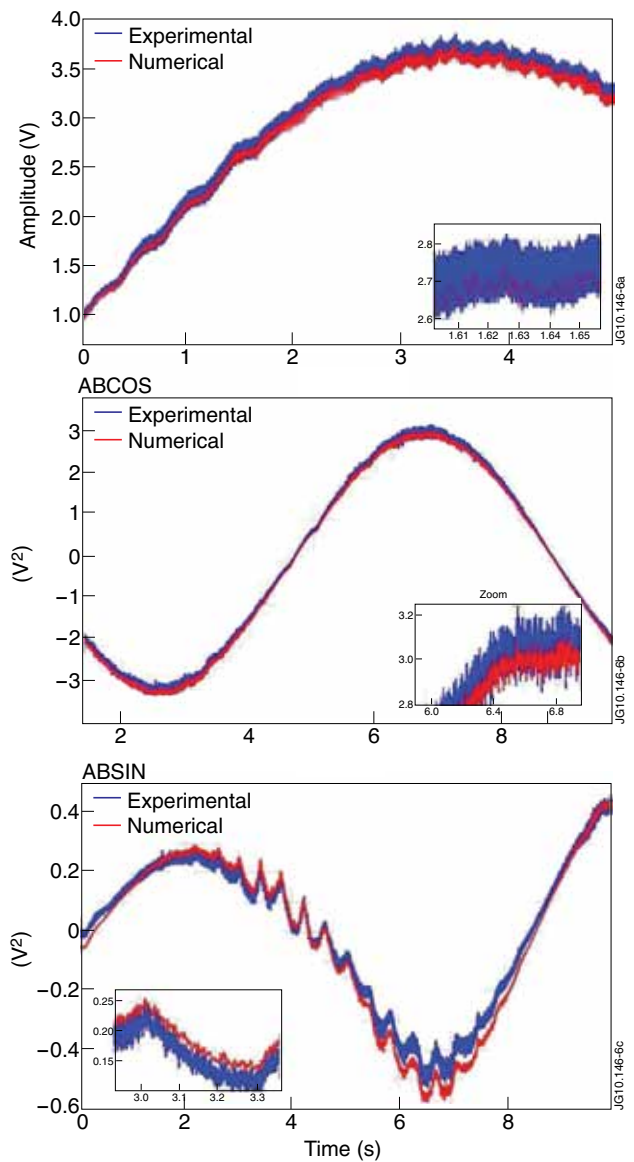
Figure 6. *Comparison between experimental data (blue) and calculation (red) for Tore Supra A, ABCOS and ABSIN signals (Channel 3).*
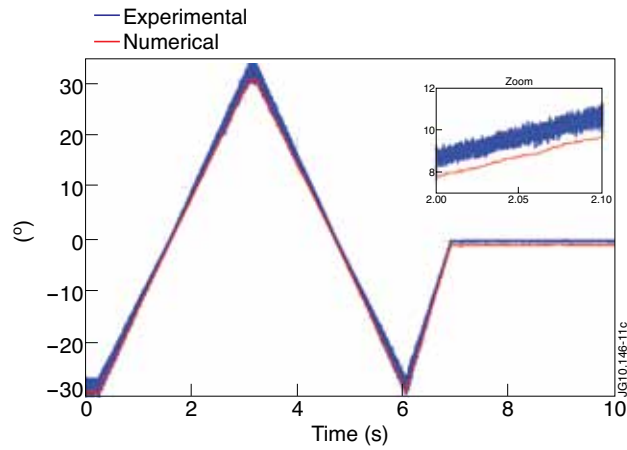
Figure 7: Comparison of the simulated and the experimental one (blue).
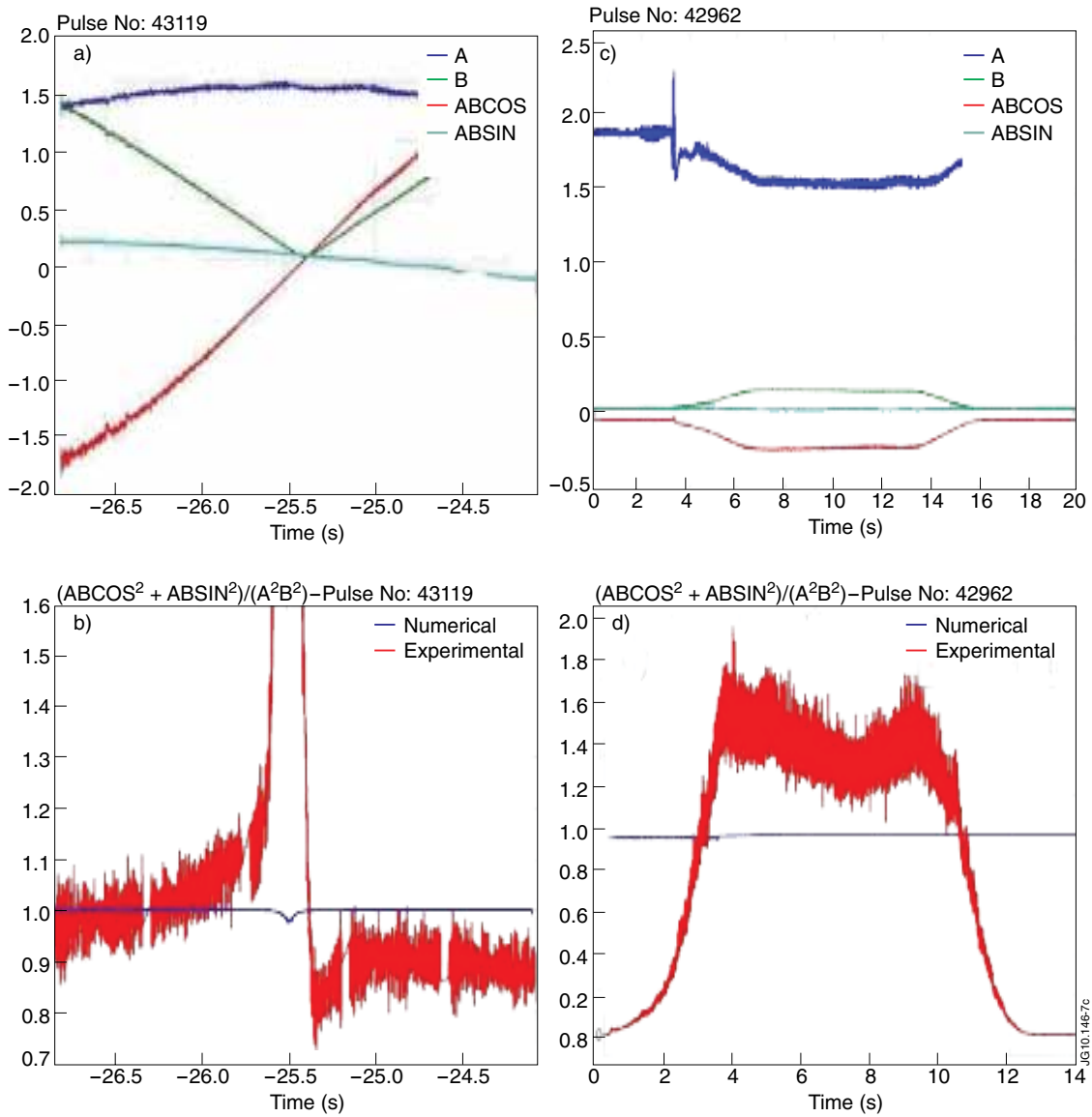
Figure 8: Conservation of (ABCOS²+ABSIN²)/A²B²=1 during a calibration (a,b) and a plasma pulse (c,d) on Tore Supra.

12
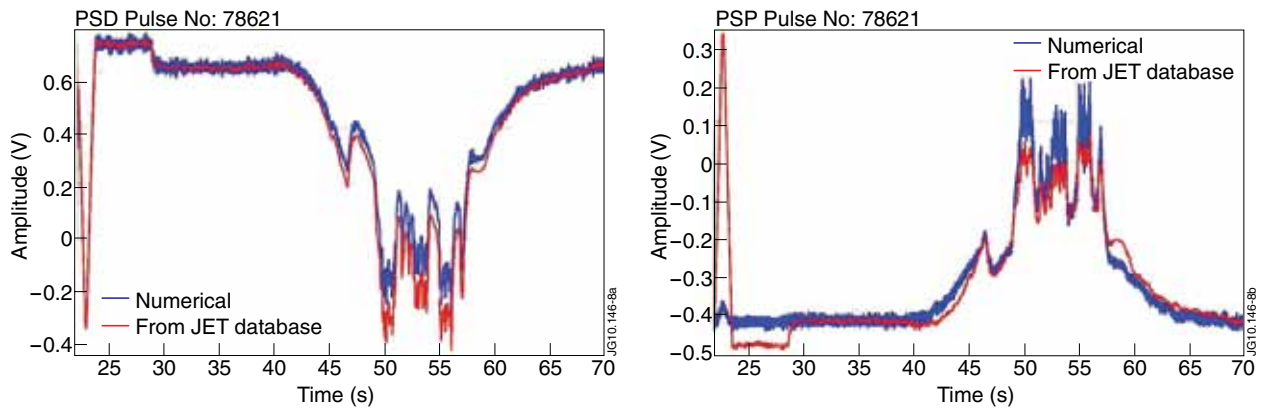
Figure 9: Comparison between Numerical (blue) and JET database signals (red) for PSD and PSP signals (Channel 3)

Figure 10: C onservation of (ABCOS²+ABSIN²)/A²B² = 1 on JET.